# Effect of Transverse Internal Ribs on Shear Strength Evaluation of Hollow RC Beams

**Ali Hameed Aziz**
Assistant Professor
Department of Civil Engineering
College of Engineering – University of Al-Mustansireah
Email: alialsaraj@yahoo.com

## ABSTRACT

**T**his paper is devoted to investigate experimentally and theoretically the structural behavior of reinforced concrete hollow beams which have internal transverse ribs under effect of shear. The number of the internal ribs is the major variable adopted in this research, while, the other variables are kept constant for all tested specimens. The experimental part includes poured and test of four (200x300x1200mm) beam specimens, three of these specimens were hollow with different locations of internal ribs and one of them was solid. The experimental results indicated that the shear strength are increased (33%) to (60%) for beams containing internal ribs in comparison with reference beam. Also, the change of beam state from hollow section to solid section led to increase the capacity for about (100%). In order to study more thoroughly the performance of tested beams, a nonlinear analysis using ANSYS-11 finite element program is used. The analytical results indicated that the load-deflection response, ultimate loads, and crack pattern are in good agreement with the experimental results.

**Key words:** shear, hollow beam, reinforced concrete, internal ribs, ansys.

تاثير الاضلاع المستعرضه الداخليه على تقييم مقاومة القص للعتبات الخرسانيه المسلحه المجوفه

**علي حميد عزيز**
استاذ مساعد
قسم الهندسه المدنيه
**كلية الهندسه ـ الجامعه المستنصريه**

**الخلاصه**

يختص هذا البحث في التحري العملي و النظري للسلوك الانشائي للعتبات الخرسانية المجوفة التي تحتوي على اضلاع بالاتجاة العرضي تحت تأثير القص. ان المتغير الرئيسي المعتمد في هذا البحث هو عدد الاضلاع الداخليه، بينما تم الابقاء على المتغيرات الاخرى ثابتة لكل العتبات المفحوصه. تضمن الجزء المختبري صب وفحص أربعة عتبات خرسانيه مسلحه بابعاد (200x300x1200 ملم) ثلاثة منها بمقاطع مجوفه تحتوي على اضلاع مستعرضه بمواقع مختلفة والاخير بمقطع صلد. اشارت النتائج المختبريه الى أن مقاومه القص ازدادت بمقدار (33%) الى (60%) للعتبات المجوفه الحاويه على اضلاع مستعرضه مقارنة مع العتبه المرجعيه. ان تغيير حالة او نوع العتبه من المجوفه الى الصلده ادى إلى زيادة التحمل الاقصى بحدود (100%). لغرض دراسة النماذج المفحوصه بشموليه أكثر، استخدم التحليل اللا خطي باستخدام برنامج العناصر المحدده (ANSYS) الإصدار-11-. اشارت النتائج التحليلية أن استجابة الانحراف-الحمل ، الحمل الاقصى، و شكل الشق في توافق جيد مع النتائج المختبريه.

**الكلمات الرئيسيه**: القص، عتبة مجوفه، الخرسانه المسلحه، الاضلاع الداخليه، البرنامج ansys

## 1. INTRODUCTION

Hollow (or box) cross section beam, mean closed thin walled section beam. A thin walled beam is characterized by relative magnitude of its dimensions; the wall thickness is small compared to the other linear dimensions of the cross section, **Abbas, 2007**. A hollow beam structure consists of top and bottom flanges connected by vertical (or inclined) webs to form a cellular section. Presence of these hollow through a solid beam eliminates a significant amount of dead space, and as a result the beam stiffness reduced and this lead to alter the simple beam behavior to a more complex one. The reduced stiffness of the beam may also give rise to excessive deflection under service load and result in a considerable redistribution of internal forces and moments. These sections are used for the various fields such that in buildings, hall, bridges, offshore structure and towers, **AL-Maliki, 2013**. It is one of the most popular forms of highway bridges; primarily because of the high flexural and torsion rigidities .The use of box beams in highway-bridge construction has proven to be a very efficient structural solution, **Al-Janabi, 2005**.

Several researches are interest in hollow beams under the effect of flexural, shear and torsion loads, **Chiad, 2013**. Shear behavior of reinforced self-compacting concrete deep box beams strengthened internally by transverse ribs, also studied, **Ruaa, 2015**. In the present research, shear behavior of reinforced concrete hollow beam strengthened internally by transverse ribs will be studied as well as the effect of the number of internal cells which were separated from each other by concrete ribs.

## 2. EXPERIMENTAL WORK

### 2.1. Experimental Program

In this paper, four simply supported beam specimens with rectangular sectional area, under monotonically concentrated load were poured and tested. The tested beams are reinforced in longitudinal direction (flexural reinforcement at the bottom), transverse direction (shear reinforcement) and have been designed to ensure failed in shear mode of failure. The number of internal cells, which were separated from each other by concrete ribs, is the major adopted variable. The sectional area, length, ratio of shear span-to-depth, flexural and shear reinforcement are kept without change for all tested beams. To evaluate the compressive strength of concrete, the experimental program consists, also, cast and test of a series of control specimens (cubes).

### 2.2. Beam Sample Details

The actual dimensions and the details of beam specimen are shown in **Fig**.1  and **Table** 1. The overall length is (1200 mm), while, the overall depth and width are (300mm) and (200 mm) respectively. All beam specimens are reinforced with ($2\phi 12$ mm) deformed bars as tension (flexural) at the bottom and ($\phi 6$ mm @150mm) deformed bars as shear reinforcement (stirrups). To hold the shear reinforcement (stirrups) in place, ($2\phi 4$ mm) smooth bars at the top are used, see **Fig**. 2.

The first beam specimen, (B-1), is poured without any internal ribs (but with two ribs at the ends), while the beam specimens (B-2) and (B-3), are poured with one and three internal ribs (in addition to two ribs at the ends) respectively. The last beam specimen, (B4), is poured without internal cells (solid). For beam specimens containing ribs (interior or at the ends), the thickness of rib is (50mm). It may be noted that the main function of the ribs at the ends is to prevent the local failure of hollow beams due to high concentration of stress near supports. While, the main

function of the internal ribs is to assist or evaluate its contribution to increase shear strength of tested beams (that have internal ribs). The locations of ribs are shown in **Figs**. 3 and 4.

The cross section of the hollow beam contains a polystyrene void that blocks out the center of the beam over specified lengths. The void is included to block out concrete where it does not add much resistance to the section and reduce the self-weight of the beam. For practical reasons, the void in the beam cross-section is obtained by a stay-in-place polystyrene block. The creation of the void through the polystyrene block makes casting the beam both time and labor intensive. There are three lengths of polystyrene block pieces as shown in **Fig**. 4.

1- One piece with length of (1100mm), for beam specimen (B-1), with one cell and one rib (50mm width), at each end of the beam.
2- Two pieces with length of (525mm) for each one of them for beam specimen (B-2), with two cells separated by three ribs (50mm width) (one internal and two at the ends).
3- Four pieces with length of (237.5mm) for each one of them for beam specimens (B-3), with four cells separated by five ribs (50mm width) (three internal and two at the ends).

## 2.3. Materials

In manufacturing the tested specimens, local construction materials are used (except steel bars), description of materials properties are reported and presented in **Table** 2.

Tensile test of steel reinforcement (manufactured in Ukraine)  is carried out on ($\phi$12mm) hot rolled, deformed, high tensile steel bar used as flexural reinforcement,  and ($\phi$6mm) deformed mild steel bar was used as stirrups (shear reinforcement). Also, the test included testing of ($\phi$4mm) plain mild steel bar which was used to hold stirrups in place. **Table** 3 shows the results of tensile test for bars.

## 2.4. Concrete Mix Design

One concrete mix is used in this work; the concrete mix proportions are reported in **Table** 4. It was found that the used mix produces good workability and uniform mixing of concrete without segregation.

## 2.5. Molds

One wooden molds containing four boxes, (200x300x1200mm) dimensions are used to poured beam specimens. The molds were manufactured with (18mm) thick plywood base and seven movable sides. The sides were fixed to the base by screws.  When the mixing process was completed, the samples were then cast in layers and compacted by a table vibrator to shake the concrete and consolidate it into the molds. Then, the top face of samples (top surface) was finished and leveled off by using steel trowel; and finally the samples were covered by a nylon sheets to impede water evaporation. It may be noted that, to ensure that it would be easy to remove the samples when the concrete hardened, the inner faces of molds was oiled.

## 2.6. Test Apparatus

Hydraulic machine was used to test the control specimens and beam specimens. Deflection at the mid-span (center) has been measured by using ELE type dial gauge of (30mm) capacity and (0.01mm) accuracy. The ELE gauge was put below the bottom face of each span at the mid. Beam profile and loading arrangement is shown in **Fig**. 5.

## 2.7. Concrete Mixing and Placing (Pouring)
### 2.7.1. Concrete mixer and vibrating table
The concrete was mixed by using a horizontal rotary mixer with (0.19 m$^3$) capacity. While, vibrating table are used to vibrate the concrete of specimens (beams and control specimens). The vibrating table consists of (1.0x1.5m) table made of (10mm) thick steel plate. The source of vibration was a rapidly rotating eccentric weight which makes the table vibrates with a simple harmonic motion. The vibrator was manufactured by Marui Company, Japan. The frequency of vibration was (7000rpm).

### 2.7.2. Curing and age of testing
After (24) hours, the beam specimens and control specimens were stripped from the molds and cured in water bath for (28) days with almost constant laboratory temperature. Before (24) hours from the date of testing, they were taken out of the water bath and tested in accordance with the standard specifications.

## 2.8. Results of Control Specimens Tests
Mechanical properties tested results of control specimens (compressive strength) are reported and summarized in **Table** 5. Cubes compressive strength ($f_{cu}$) was carried out on concrete based on BSI **881-116** with standard cubes (150mm). The cubes were loaded uniaxially by the universal compressive machine up to failure.

## 2.9. Test Methodology (Test Procedure)
The beams were tested at (28 days) age, where they were prepared by cleaning them and paint with white color, in order to detect the propagation of cracks. The beam specimens have been placed on the testing machine with a clear span of (1100mm), then adjusted to fit the supports, beam centerline, dial gauge and finally tested under a monotonic single-point loading up to failure; **Fig**. 5 shows the setup of beam specimens.

Initially each beam is loaded with small load to ensure that the dial a gauge is in touch with the bottom faces of beams and working correctly. After that, the load increased regularly at (1.0 kN/sec) and the readings taken every (5 kN). When the beams reached advanced stage of loading, smaller increments of load were applied until failure, as the load indicator stopped in recording or returned back and the deflection increased very fast without any increase in applied load. Throughout the test, all necessary measurements and notices were recorded.

## 3. THEORETICAL STUDY
To study the performance of tested beams, ANSYS (Version-11) finite element program is used to analyze two selected beam specimens, (B-1) and (B-2). A nonlinear, eight nodes brick element, (SOLID-65), with three translations DOF at each node is used to model the concrete. For FEM modeling of the steel reinforcement, two nodes, discrete axial element, (LINK-8), with three translations DOF at each node is used. To avoid stress concentration, (10mm) thick steel plate is added at the load locations and modeled by using a nonlinear, eight nodes brick element, (SOLID-45), with three translations DOF (per node) in x, y and z-directions.

## 3.1. Properties of Materials
3.1.1. Concretes
For finite element modeling, concrete constitutive stress-strain curve in compression can be described by isotropically, multi-linear stress-strain relationship. Constitutive model (surface

of failure) in ansys can be specifying only by two constants (tensile strength ($f_t$) and compressive strength of concrete ($f_c'$)) as given by criterion of **Willam** and **Warnke, 1975**.

In this paper, transfer coefficients of shear for opened cracks ($\beta_o$) and closed cracks ($\beta_c$) are assumed to be (0.2) and (0.25) respectively. These values are selected to avoid convergence problems during iteration.

The stress-strain curve for concrete in tension is assumed to be linear-elastic up to the maximum tensile strength. Smeared crack approach is used to model the concrete cracking. Poisson's ratio, for finite element modeling of concrete is assumed to be (0.2). In order to modeling the finite element of concrete, empirical equations of ACI-318 Committee are used to determine the young's modulus and tensile strength, as listed in **Table** 6.

### 3.1.2. Steel Plates and Reinforcement

Elastic modulus and yield stress for the steel plates and reinforcement used in FEM follow the design material properties used for the experimental investigation. The steel for the finite element models is assumed to be an elastic-perfectly plastic with strain hardening material and identical in tension and compression as shown in **Fig**. 6. Von-Mises failure criterion is adopted for modeling. To avoid convergence problems during program iteration, the modulus of strain hardening is assumed to be (0.03x $E_s$).

The steel plate under the applied load is assumed to be behaves as linearly-elastic materials. Young's modulus of (200GPa) and Poisson's ratio of (0.3) are utilized in FEM for steel plates and reinforcement.

## 3.2. Finite Element Modeling

The dimensions of the beam specimens are shown in Fig. 1. Due to variation of internal ribs locations and simple geometry of the tested beams, entire (full) beam is used for modeling, **Fig**. 7.

It may be noted that, the origin point of coordinates lie in one corners and only one loading plate are provided at the top of beam (under load) to prevent load concentration.  In the beginning, the beams and steel plates are modeled as lines, then areas, and finally as volumes (solid elements).

### 3.2.1. **Finite element meshing**

After creating of volumes, meshing of the finite element model is needed. In this stage, the FEM model is divided into a number of small elements. When the model problem is solving, the stresses and deformations (strains) are estimated at the Gaussian points of these small elements. Best results can be achieved by dived (meshing) the model into square (or rectangular) elements, **Fig**. 7.

Before distribution (spreading) of the applied load by using steel plates (in the early attempt), and due to load concentration on concrete elements, concrete crushing started to create in elements which located directly under load. Thereafter, the concrete elements adjacent to the applied load were crushed within few steps of loading. Finally, large displacement (deflection) take place, the solution in not converges and as a result the FEM model failed prematurely. To prevent this FEM failure phenomenon, steel plates are used and inserted under the applied load.

15

3.2.2. **Load application and boundary conditions**

To ensure that modeled beams behave as tested beams, boundary conditions (displacement constrains) at supports should be satisfied (need to be applied at the supports locations). Thereafter, one of the supports is to be modeled as a hinge and the other one is modeled as a roller.

Since the external load was applied on a steed plate and as a basic of FEM, the plate load must be transformed to adjacent nodes; therefore the applied load is represented by an equivalent nodal force on the top nodes of plate. Since the steel plate had eight divisions in transverse direction (Z-direction), the equivalent nodal force on the plate becomes (P/9) of the applied force (assuming equally distributed of applied load).

The applied load is divided into load steps and done incrementally up to failure (based on Newton-Raphson technique). At a certain stages in the analysis, load step size is varied from large (at points of linearity in the response) to small (when cracking and steel yielding occurred). The failure is assumed to be occurred when the solution, for a minimum load is diverging and the models have a large deflection (rigid body motion).

## 4. RESULTS AND DISCUSSIONS

As indicated before, the aims of this paper are to evaluate the effect and contribution of internal ribs (at different locations) on shear strength of hollow reinforced concrete beams.

### 4.1. Experimental Results

Ultimate load capacities, load versus deflection at the center of the bottom face of each tested beam were recorded throughout the experimental work. To appear the cracks pattern and imported details, photographs for the tested specimens are taken. Tests observations, general behavior and recorded data are reported to recognize and understand the effects of adopted parameters on the strength of the tested specimens.

4.1.1. **General behavior**

Photographs of the tested beams are shown in **Fig. 8** and tests results are given in **Table 7.** It may be noted that, all beam specimens were designed to be failed in shear, which was distinguished by sudden failure and diagonally wide cracks which extend from supports towards the applied load locations.

The general behavior of the tested beams can be described as follows; at early stages of loading, small vertical deflection initiated in the mid span of tested beams, with further loading, diagonal cracks extended upwards and became wider in shear span. One or more cracks propagated faster than the others and extend through weak locations in the beam (hollow zones) and reached the compression face (near applied load), where crushing of the concrete near the positions of applied loads had occurred due to high concentrated stresses under load.

4.1.2. **Failure mode**

The appearance of the cracks reflects the failure mode for the tested beams. The experimental evidences show that the diagonal cracks extended horizontally along the tension reinforcement and eventually, the failure take place due to diagonal tension cracks were formed diagonally and moved up and towards the position of load, this crack is associated with crushing of the concrete near the positions of applied loads, this mode of failure is called "Shear-Compression" failure, as shown in **Fig**. 8.

4.1.3. **Ultimate shear strength (Vu)**

The recorded ultimate loads of the tested beams are presented in **Table 7**. As expected, test results show that the reference beam (B-1) has the minimum ultimate strength in comparison with the rest beams. This may be due to absent of any internal ribs (concrete) in the section (in shear span).

As shown in **Table** 7, the ultimate shear strength increased when the number of ribs increased (in shear span) and when we moved toward of and closes up to the support.

For the tested beam (B-4), which have made as solid without hollows, the ultimate shear strength increased by (100%) in comparison with reference beam, this clearly due to concrete contribution to resist shear stress.

The ultimate shear strength increased about (33%) to (60%) for the tested beams (B-2) and (B-3) respectively, the presence of internal ribs led to increase resistant area of concrete and as a results, the shear strength increased significantly.

### 4.1.4. Effect of number of ribs on ultimate strength

As shown in Table (7), presence of internal ribs in hollow section leads to increases the stiffness of tested beams due to concrete contribution, and this leads to increase in carrying capacity.

In other words, due to abrupt changes in the sectional configuration (from solid to hollow), the hollow beam corners, closed thin webs and flanges are subject to high stress concentration that may lead to reduction in stiffness of the tested beam and produced cracking and excessive deflection, see **Fig**. 9.

As shown in **Table** 7, presence of internal ribs (see B-2 and B-3), led to increase the ultimate shear strength from (33%) to (60%).  The increasing in ultimate load was (100%) for tested beam (B-4) when the section made fully without hollows. This means that the presence of internal ribs affected significantly on ultimate capacity of tested beams.

### 4.1.5. Load versus deflection curves

Load versus deflection curves of the tested beam specimens at the center of bottom face at all loading increments up to failure are shown in **Fig**. 9.

In the beginning, the curves are identical and the tested beams exhibited linear behavior and the initial change of slope of the load-deflection curves occurred between (10 kN to 30kN), which may be indicated the first crack loads. Beyond the first crack loading, each beam behaved in a certain manner. Behavior of reference Beam (B-4) exhibited greater loads and smaller deflections in comparison with the other beams. This beam had the greatest stiffness due to absent of any hollows.

Load-deflection curves for the tested beams (B-1, B-2 and B-3) shows smooth increase, in both, applied loads and deflection. Presences of hollows lead to decreasing in carrying capacity of load beyond the first cracking, this associated with reduction in beams stiffness and this is reflected on the associated deflection (excessive deflection). For tested beams (B-1 and B-2), slight increase in ultimate deflection of beam (B-1) is observed by comparing with (B-2). This is may be due to absent of any interior rib in the beam (B-1) which leads to decreasing of beam rigidity (stiffness) and as a result, slight increases in deflection is occurred.

### 4.2. Finite Element Results
### 4.2.1. Load versus deflection curves

Vertical displacements (Deflection in y-direction) are measured, at mid-span, at the center of the bottom face of tested beams. Deflected shape of finite element beam model due to the vertical load is shown in **Fig**. 10. The load versus deflection curves obtained from the FEM

analysis together with the experimental tests are constructed and compared in **Fig**. 11, for tested beams (B-1) and (B-2). In general, it can be noted from the load-deflection curves that the finite element analyses are agree well with the experimental results throughout the entire range of behavior. Comparing with the experimental results, all the finite element models show relatively large capacity at the ultimate stage.

### 4.2.2. Ultimate loads

Table 8 shows the comparison between the ultimate loads of the experimental (tested) beams, $(P_u)_{EXP.}$, and the final loads from the finite element models, $(P_u)_{FEM}$. The final loads for the finite element models are the last applied load steps before the solution starts to diverge due to numerous cracks and large deflections.

As shown in **Table** 8, the ultimate loads obtained from numerical model agree well with the corresponding values of the experimental (tested) beams.

### 4.2.3. Crack patterns

The crack pattern is recorded, after first crack, at each load step. Cracks pattern come by the FEM analysis and the failure modes of the tested beams are agree well, as shown in **Fig**. 12.

Cracks pattern appearances reflect the failure mode of tested specimens. The model of FEM, accurately, predicts that the tested beams are failing in shear and predicts that the vertical and inclined cracks formed in the shear span regions respectively. The cracks are concentrated under load region and vanish diagonally towards the beam supports.

### 5. CONCLUSIONS

In the previous items, an experimental program together with finite element analysis has been performed, thereafter the following conclusions are obtained:-

1-Ultimate load carrying capacity in beams is found to be increasing with increase the number of the internal ribs, and the deflection at ultimate load is found to be decreasing.

2-The ribs work as internal stiffeners which contributed to increase the shear strength in a certain degree. The shear strength increased (33%) and (60%) for beams containing one and three internal ribs respectively.

3-The change of beam state from hollow section to solid section led to increase the capacity for about (100%).

4-Based FEM analysis (using ANSYS program), it can be concluded that the computational finite element models adopted in the current study are useful and able to simulate the behavior of tested beams. The analytical tests indicated that the load-deflection responses, ultimate loads and the structural behavior are in good agreement with the experimental results.

### 6. NOMENCLATURE

$b_w$ =   beam width, m.
$h$ =   overall depth of beam, m.
$d$ =   effective depth, m.
$f_c^{'}$ =   cylinder compressive strength of concrete, MPa.
$f_{cu}$ =   cube compressive strength of concrete, MPa.
$f_t$ =   tensile strength of concrete, MPa.
$f_y$ =   yield strength of steel bars, MPa.

$f_u$=      ultimate tensile strength of steel bars, MPa.

$E_c$=      modulus of elasticity of concrete, MPa.

$E_s$=      modulus of elasticity of steel, MPa.

$P_c$ =      cracking load, kN.

$P_u$ =      ultimate load, kN.

$V_u$=      ultimate Shear Force, kN.

$(V_u)_i$=      ultimate Shear Force of a certain beam, kN.

$\phi$ =      reinforced bar diameter,mm.

$\beta_c$      shear transfer coefficient for closed cracks.

$\beta_o$      shear transfer coefficient for open cracks.

## REFERENCES

➢ Abbas, H. E., 2007, *Nonlinear Analysis of Prestressed Concrete Box Section Beams*, M.Sc. Thesis, Department of Civil Engineering, University of Al-Nahrain.

➢ ACI Committee 318, 2008, *Building Code Requirements for Structural Concrete (ACI 318-08 M) and commentary,* American Concrete Institute, Farmington Hills, MI, USA, 430pp.

➢ AL-Maliki, H. N., 2013, *Experimental Behavior of Hollow Non-Prismatic Reinforced Concrete Beams Retrofit With CFRP Sheets*, Journal of Engineering and Development, Vol. 17, No.5, November, pp(224- 237).

➢ AL-Janabi, W.A., 2005, *Analysis and Shape Optimization of Varied Section Box Girder Bridges*, M.Sc. Thesis, Department of Civil Engineering, University of Tikrit.

➢ *ANSYS Manual*, Version (11).

➢ BS1881-116, 1983, *Method for Determination of Compressive Strength of Concrete Cubes*, British Standards Institute, London.

➢ Chiad, S. S., 2013, *Shear Stresses of Hollow Concrete Beams*, Journal of Applied Sciences Research, Vol. (9), No.(4),pp.(2880-2889).

➢ Iraqi Specifications No. (5),1984, *Portland Cement*, the Iraqi Central Organization for Standardization and Quality Control, Baghdad-Iraq.

➢ Iraqi Specifications No. (45),1984, *Aggregates from Natural Sources for Concrete and Building Construction*, the Iraqi Central Organization for Standardization and Quality Control, Baghdad-Iraq.

➢                                                                          Ruaa Y. H., *2015, Shear Behavior of RC Deep Box Beams Strengthened Internally by Transverse Ribs,* M.Sc. Thesis, College of Engineering, Civil Engineering Department, Al-Mustansiria University, Baghdad, Iraq.

➤ Willam, K., and Warnke, E.,1975, *Constitutive Model for the Triaxial Behavior of Concrete*, Proceedings, International Association for Bridge and Structural Engineering, Vol. (19), ISMES, pp. 174, Bergamo, Italy.
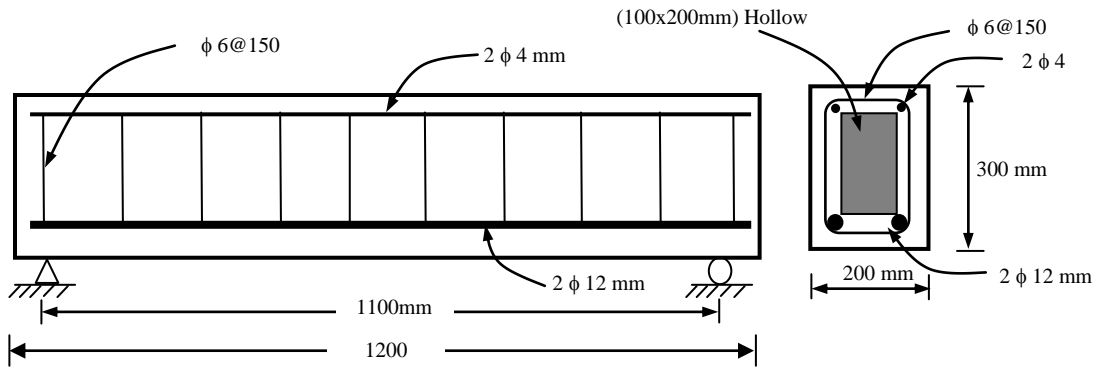


**Figure 1.** Details of tested beams.



**Figure 2.** Details of reinforcement.



**Figure 3.** Details of polystyrene blocks (inside mold).
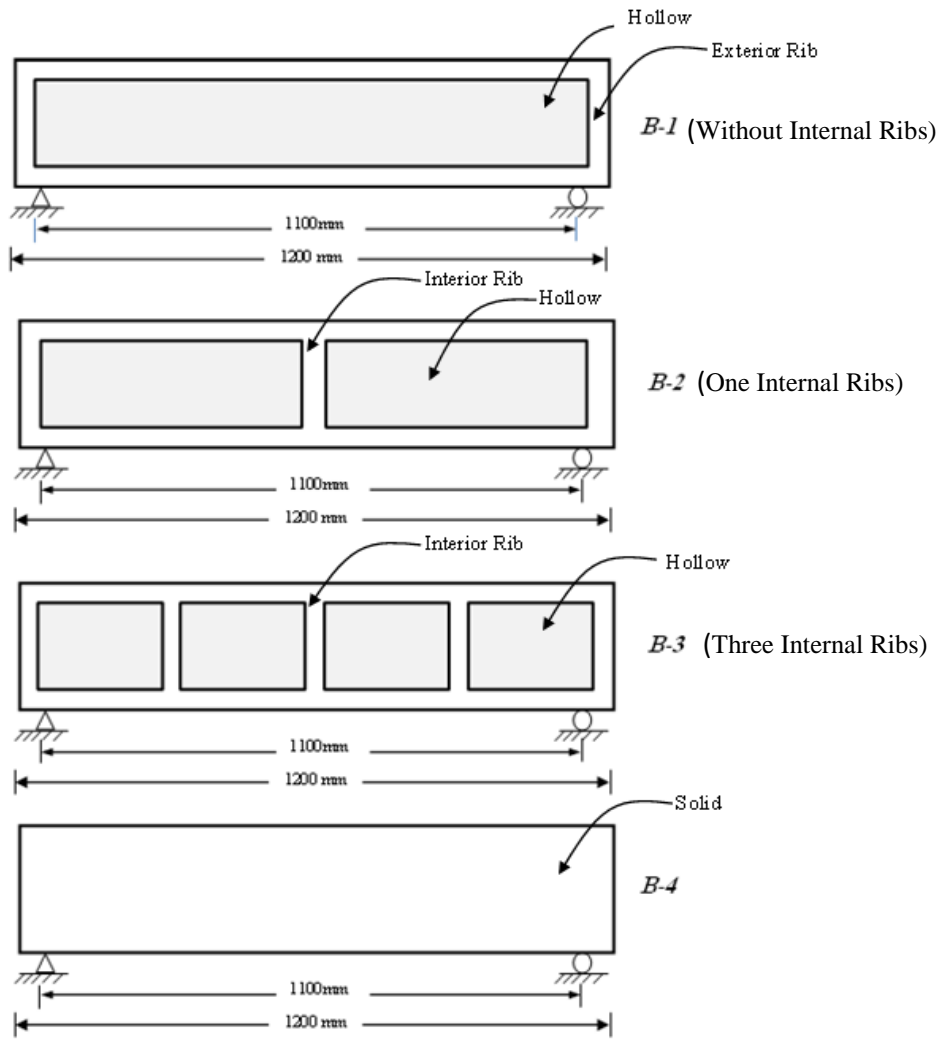
**Figure 4.** Locations of external and internal ribs (longitudinal section).



**Figure 5.** Beam specimen setup.
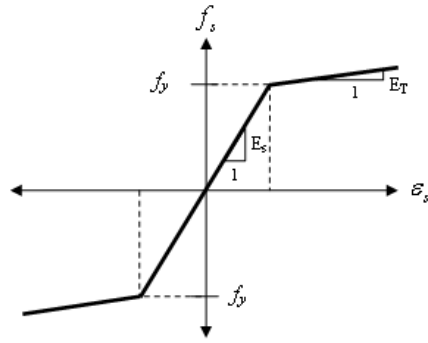
**Figure 6.** Modeling of steel materials.
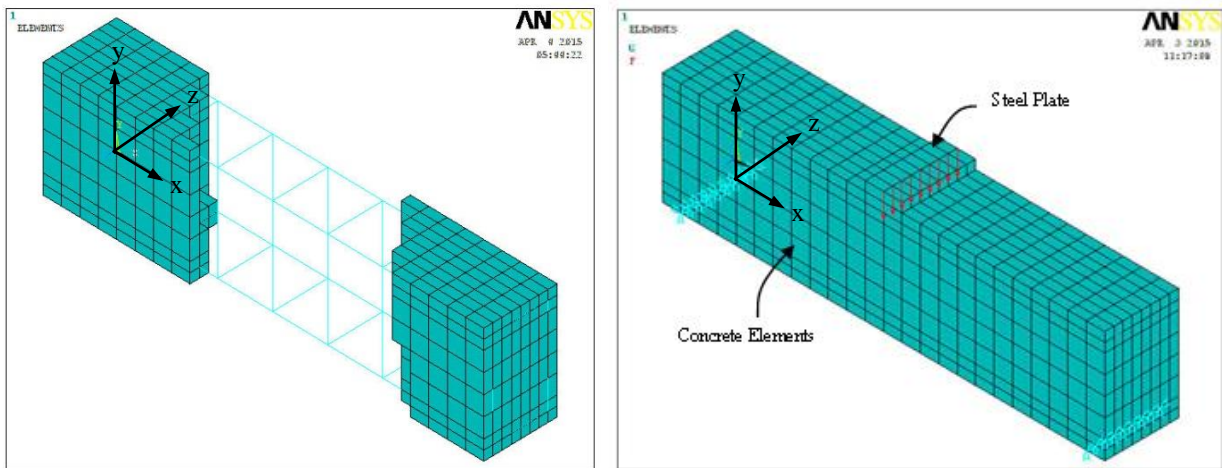


**Figure 7.** Mesh of the concrete and steel plate.
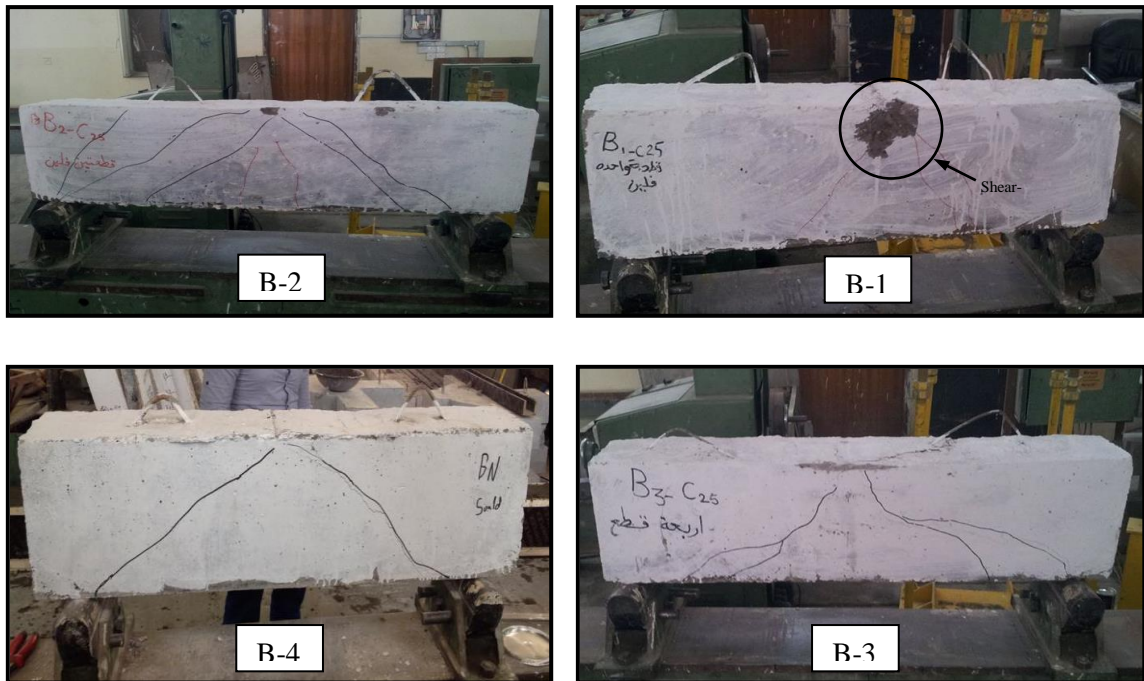


**Figure 8.** Crack patterns of tested beams.
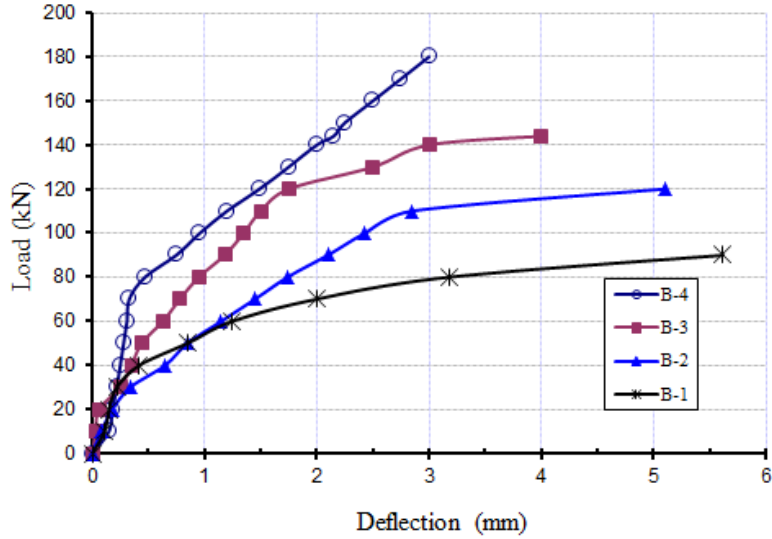
**Figure 9.** Load-deflection relationship of tested beams.
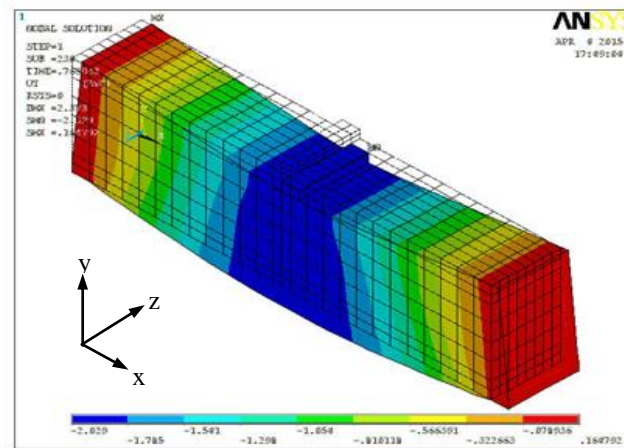


**Figure 10.** Deflected shape of beam model.
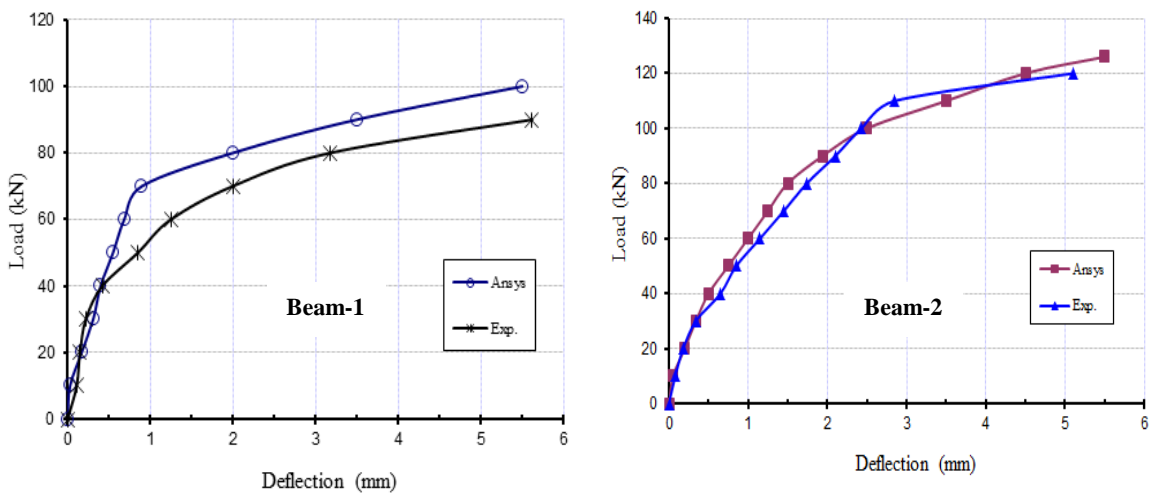


**Figure 11.**  Load-deflection relationship for beam (B-1) and beam (B-2).
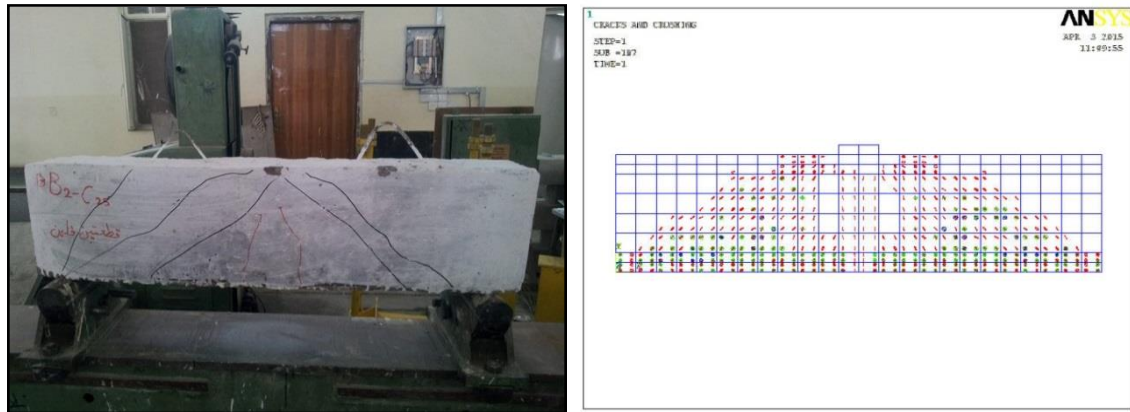
**Figure 12.** Crack pattern from FE model (right) and experimental tests (left) for B-2.

**Table 1.** Beams designation and details.

| Beam Designation | Dimensions (mm) | | | Reinforcement | | Transverse Ribs ** |
|---|---|---|---|---|---|---|
| | $b_w$ | $h$ | $l$ | Flexural | Shear | |
| (B-1)* | | | | | | Two (At Ends Only) |
| B-2 | 200 | 300 | 1200 | $2 \phi 12$ mm | $\phi 6$ mm @150mm | Three Ribs |
| B-3 | | | | | | Five Ribs |
| B-4 | | | | | | Without Ribs (Solid) |

*Reference Beam                    **(50mm) thickness

**Table 2.** Construction materials description.

| Material | Descriptions |
|---|---|
| Cement* | Ordinary Portland Cement (Type I) |
| Sand** | Natural sand from Al-Ukhaider region with maximum size of (4.75mm) |
| Gravel** | Crushed gravel with maximum size of (12mm) |
| Water | Clean tap water (used for both mixing and curing) |

* Conform to **Iraqi specification No. 45/1989**.      ** Conform to **Iraqi specification No. 45/1984**.

**Table 3.**  Steel bars properties.

| Nominal Diameter (mm) | Bar Type | $f_y$* (MPa) | $f_u$ (MPa) | Elongation % |
|---|---|---|---|---|
| 4 | Plain | 461 | 633 | 16 |
| 6 | Deformed | 383 | 545 | 11 |
| 12 | Deformed | 860 | 915 | 16 |

**\*** Average of three samples (Each 400mm length)

**Table 4.** Proportions of concrete mix.

| Parameter | Quantity |
|-----------|----------|
| Water/cement ratio | 0.40 |
| Water | 168 Liter |
| Cement | 420 kg/m$^3$ |
| Fine Aggregate | 600 kg/m$^3$ |
| Coarse Aggregate | 1200 kg/m$^3$ |

**Table 5.** Mechanical properties of concrete

| Property (MPa) | Value (MPa) |
|----------------|-------------|
| Cube compressive strength ($f_{cu}$) [*] | 30 |
| Cylinder compressive strength ($f_c^{'}$) [**] | 24.6 |

*Average of three samples.     ** $f_c^{'} = 0.82 f_{cu}$

**Table 6.** Modulus of elasticity and tensile strength adopted in FEA.

| Empirical Equation | $f_c^{'}$ (MPa) | Value (MPa) | Note |
|--------------------|-----------------|-------------|------|
| $E_c = 4700\sqrt{f_c^{'}}$ | 24.6 | $E_c = 23311$ | ACI-318 |
| $f_t = 0.62\sqrt{f_c^{'}}$ |  | $f_t = 3.08$ |  |

**Table 7.** Ultimate shear strength of tested beams.

| Beam Designation | $P_u$ (kN) | $P_c$ (kN) | $V_u$ (kN)** (kN) | $(V_u)_i/(V_u)_R$ (%) | Mode of Failure |
|------------------|-----------|-----------|-------------------|-----------------------|-----------------|
| (B-1)* | 90 | 15 | 45 | 1.0 | Shear-Compression |
| B-2 | 120 | 20 | 60 | 1.33 | Shear-Compression |
| B-3 | 144 | 24 | 72 | 1.6 | Shear-Compression |
| B-4 | 180 | 25 | 90 | 2.0 | Shear-Compression |

*Reference Beam     ** $V_u = P_u/2$

**Table 8.** Comparison between experimental and finite element ultimate loads.

| Beam Designation | Ultimate Load (kN) | | $\dfrac{(P_u)_{FEM}}{(P_u)_{EXP.}}$ |
|------------------|---------------------|-----------------|-------------------------------------|
|  | $(P_u)_{EXP.}$ | $(P_u)_{FEM}$ |  |
| B-1 | 90 | 99 | 1.1 |
| B-2 | 120 | 126 | 1.05 |